Field experiment on sound propagation from an elevated directional source

Shinichi Sakamoto[1]; Toshikazu Takanashi[2]; Sakae Yokoyama[3]; Hirokazu Ishii[4]

[1] Institute of Industrial Science, The University of Tokyo, Japan

[2] INC Engineering Co., Ltd., Japan

[3] Kobayasi Institute of Physical Research, Japan

[4] Japan Aerospace Exploration Agency, Japan

ABSTRACT

The authors investigate outdoor sound propagation from a directional source by field experiments. Results on ground-to-ground sound propagation are reported in this conference by another paper. In addition to an experimental investigation on ground-to-ground sound propagation from a directional source, in this report, results of an experiment on air-to-ground sound propagation from an elevated directional source lifted by a tethered balloon is described. In this experiment, a horn type loudspeaker was raised at the heights of about 100 and 200 m, and sound propagation characteristics from the source to receivers on the ground were analyzed from impulse responses measured by a swept sine method. As a result of the experimental study, which was made under a meteorologically calm condition, it was confirmed that the sound propagation characteristics can be accurately estimated by considering the directivity characteristics of the sound source in low and middle frequencies, and that they are considerably affected by meteorological effects.

Keywords: Outdoor sound propagation, Swept-sine method

I-INCE Classification of Subjects Number(s): 24.6

1. INTRODUCTION

Long-range outdoor sound propagation is strongly affected by meteorological effect due to vertical distribution of wind and temperature. Many researches have been made on the long-range outdoor sound propagation by field measurements and numerical analyses. Although noise sources outdoor including aircrafts, ground vehicles and railroad trains are directional, many studies assume omnidirectional characteristics as the sound sources. Focusing on the effects of source's directionality, therefore, the authors made field experiment on outdoor sound propagation from directional sources of which directional characteristics are known. In this report, sound propagation characteristics from an elevated source to receivers near ground (air to ground propagation) are described, whereas the other report shows experimental results on ground to ground propagation (1). The experimental results are compared with those obtained by simple calculation methods in order to see the specific features of the air to ground sound propagation. Furthermore, a precise computation based on the Green's Function Parabolic Equation (GF-PE) method is applied to calculate the sound propagation from a directional source. The calculation results are compared with the experimental results, and the validity of the calculation method is investigated.

2. FIELD EXPERIMENT

Field experiment on outdoor sound propagation was performed at Taiki Aerospace Research Field in Hokkaido Japan. The experimental field has a straight runway of 1 km long and 60 m wide treated

[1] sakamo@iis.u-tokyo.ac.jp
[2] t_takanashi@inc.ihi.co.jp
[3] sakae@kobayasi-riken.or.jp
[4] ishii.hirokazu@jaxa.jp

with dense asphalt pavement surrounded by a grass field. On a centerline of the runway, 11 receiving points were lined up with equal intervals of 100 m. Arrangement of the receiving points on the runway are shown in Fig. 1. At the receiving points, 1/2 inch condenser microphones were set at their heights of 1.2 m. In order to grasp the vector wind condition of the field, ultrasonic anemometers capable of measuring wind speed and direction in a horizontal plane were set at 1.2 m high and 5 m high, at three points (center position of the runway and ±300 m from the center position, as shown in Fig. 1). As a sound source, a horn-type directional loudspeaker shown in Fig. 2 was hanged by a tethered balloon. The directional characteristics of the horn-type loudspeaker were measured in advance of the field measurement as shown in Fig. 3.

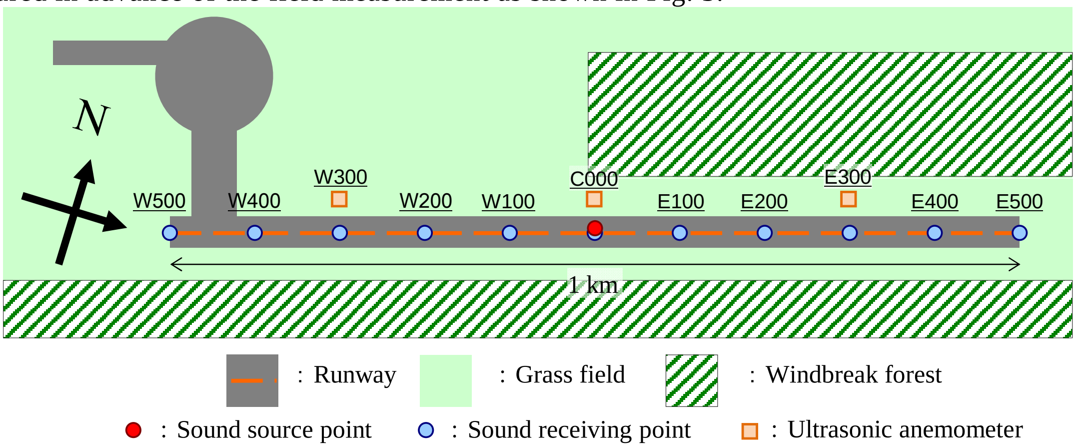

Figure 1 – Arrangement of receiving points on runway.

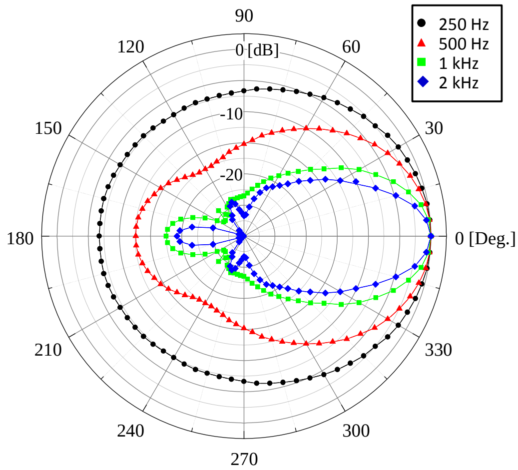

Figure 2 – Directional loudspeaker Figure 3 – Directional characteristics of the loudspeaker

The sound source was set under the balloon so that the angle formed by the radiation direction of the loudspeaker and the gravity direction becomes 45 degrees. The balloon was tethered to a winch set at a vicinity point of the center of the runway as shown in Fig. 4, and was lifted up at heights of 93 m and 200 m. In order to grasp sound propagation from the elevated source to the receiving points, impulse responses were measured using swept-sine signals with the frequency range from 250 Hz to 2 kHz for 1 minute to secure sufficient sound energy to measure the long-range sound propagation (2). At the receiving points, C-weighted sound pressure signals from sound level meters and GPS signals for synchronization were recorded by 2-channel linear PCM recorders at the sampling frequency of 22050 Hz. At the same time of the recording the signal, the elevated balloon and the loudspeaker were video recorded to know their relative rotation angle to the runway. Azimuth angle of the balloon and the loudspeaker which was determined by confirming the recorded video, during swept-sine signals were radiated, is shown in Fig. 5. From all of recorded samples, adequate samples for analysis in which the azimuth angle of the loudspeaker directed to almost the east or the west (the runway direction) were eliminated in order to analyze the sound propagation characteristics. Figure 6 shows vector wind speed in westbound direction. As is seen from the figure, the operation of the balloon began at almost no wind condition and ended when it breezed up, and the total time of the operation was around two hours.

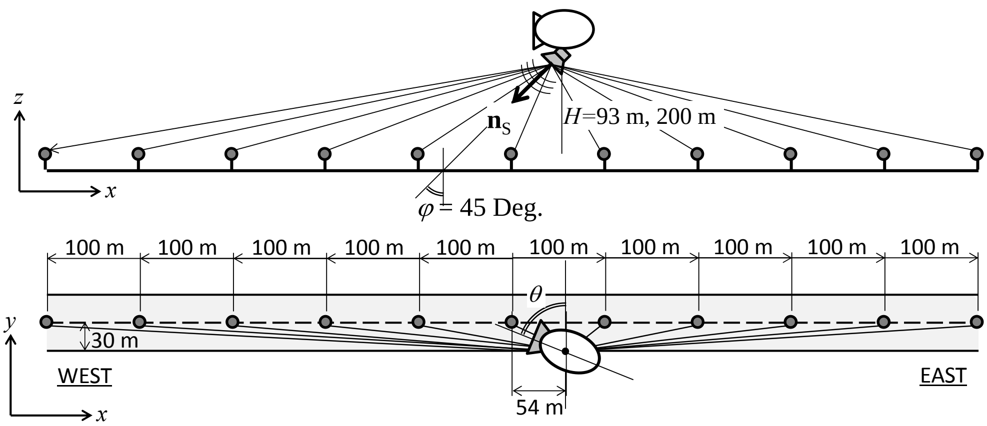

Figure 4 – Geometrical relationship between elevated source and receiving points.

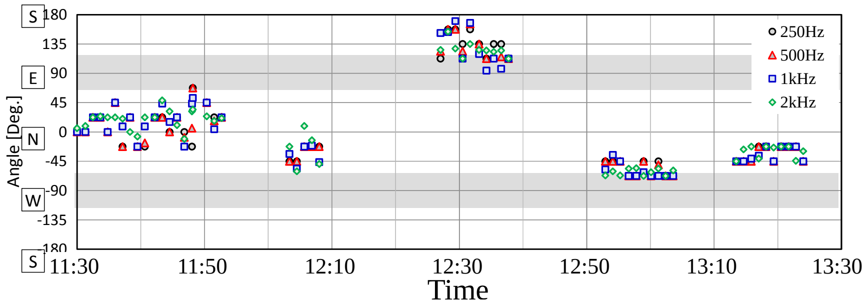

Figure 5 – Azimuth angle of balloon lifting the loudspeaker used as the sound source.

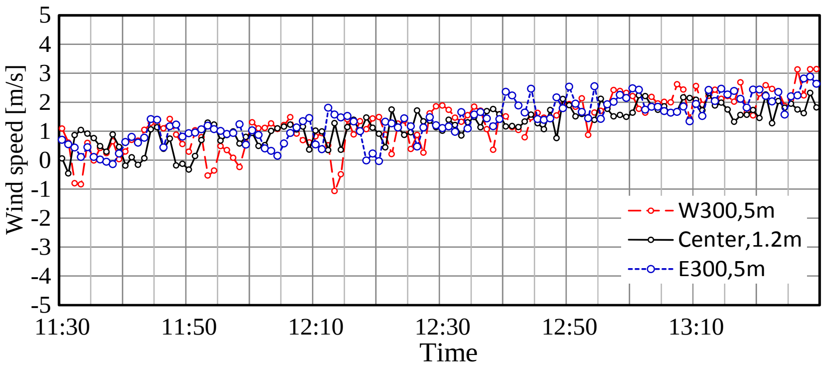

Figure 6 – Vector wind on measuring Air to Ground sound propagation.

3. SIMPLE CALCULATION OF SOUND PROPAGATION

In order to compare with the experimental results, sound propagation was calculated by the following simple two methods; the one is an energy-base calculation (Method 1) and the other is a wave-base calculation including interference effect between direct sound and ground reflection (Method 2).

3.1 Method 1: Energy-base calculation considering directivity

By the Method 1, sound pressure level at the receiving point is simply calculated by considering distance attenuation and a directivity of the loudspeaker in energy-base as,

$$\Theta = \cos^{-1}\left(\frac{\mathbf{n}_S \cdot \mathbf{r}}{|\mathbf{r}|}\right) \tag{1}$$

$$L = L_0 - 10\log_{10}\left(\frac{r}{r_0}\right) + 10\log_{10}|Q(\Theta)|^2 \tag{2}$$

where $\mathbf{r}$ indicates a vector pointing from the source located at (x_S, y_S, z_S) to a receiving point (x_R, y_R, z_R) and is calculated as $\mathbf{r} = (x_R - x_S, y_R - y_S, z_R - z_S)$. $\mathbf{n}_S$ indicates a pointing vector of radiation direction of the loudspeaker and is calculated as $\mathbf{n}_S = (\sin\varphi\cos\theta, \sin\varphi\sin\theta, \cos\varphi)$ using the depression angle φ and azimuth angle θ (see Fig. 4). L_0 indicates sound pressure level at a reference distance r_0 in a free field, r is the distance between the source and the receiver, $Q(\Theta)$ is directivity coefficient of the loudspeaker.

3.2 Method 2: Wave-base calculation considering directivity and reflection by the ground

By the Method 2, sound pressure is calculated in wave-base to consider sound interference between direct sound and ground reflection. As shown in Fig. 7, a mirror image of a receiver is considered, and the sound pressure at the receiver is calculated as a summation of contributions of sound pressure from the source to the real receiver and the image receiver as,

$$p = Q(\Theta)\cdot\left(10^{\frac{L_0}{10}}\right)\cdot\left(\frac{e^{-jk|\mathbf{r}_{\mathrm{R,r}}|}}{|\mathbf{r}_{\mathrm{R,r}}|} + R\frac{e^{-jk|\mathbf{r}_{\mathrm{R,m}}|}}{|\mathbf{r}_{\mathrm{R,m}}|}\right) \qquad (3)$$

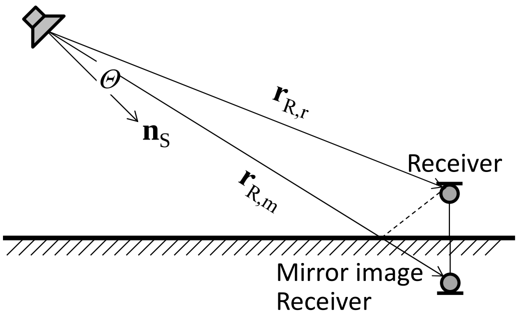

Figure 7 – A real and mirror receivers for calculation by the Method 2.

where k is a wavenumber, $\mathbf{r}_{\mathrm{R,r}}$, $\mathbf{r}_{\mathrm{R,m}}$ are pointing vectors from the source to a real receiver and to an image receiver, respectively. R indicates a complex reflection coefficient, and is assumed R=1.0 for simplicity in this investigation.

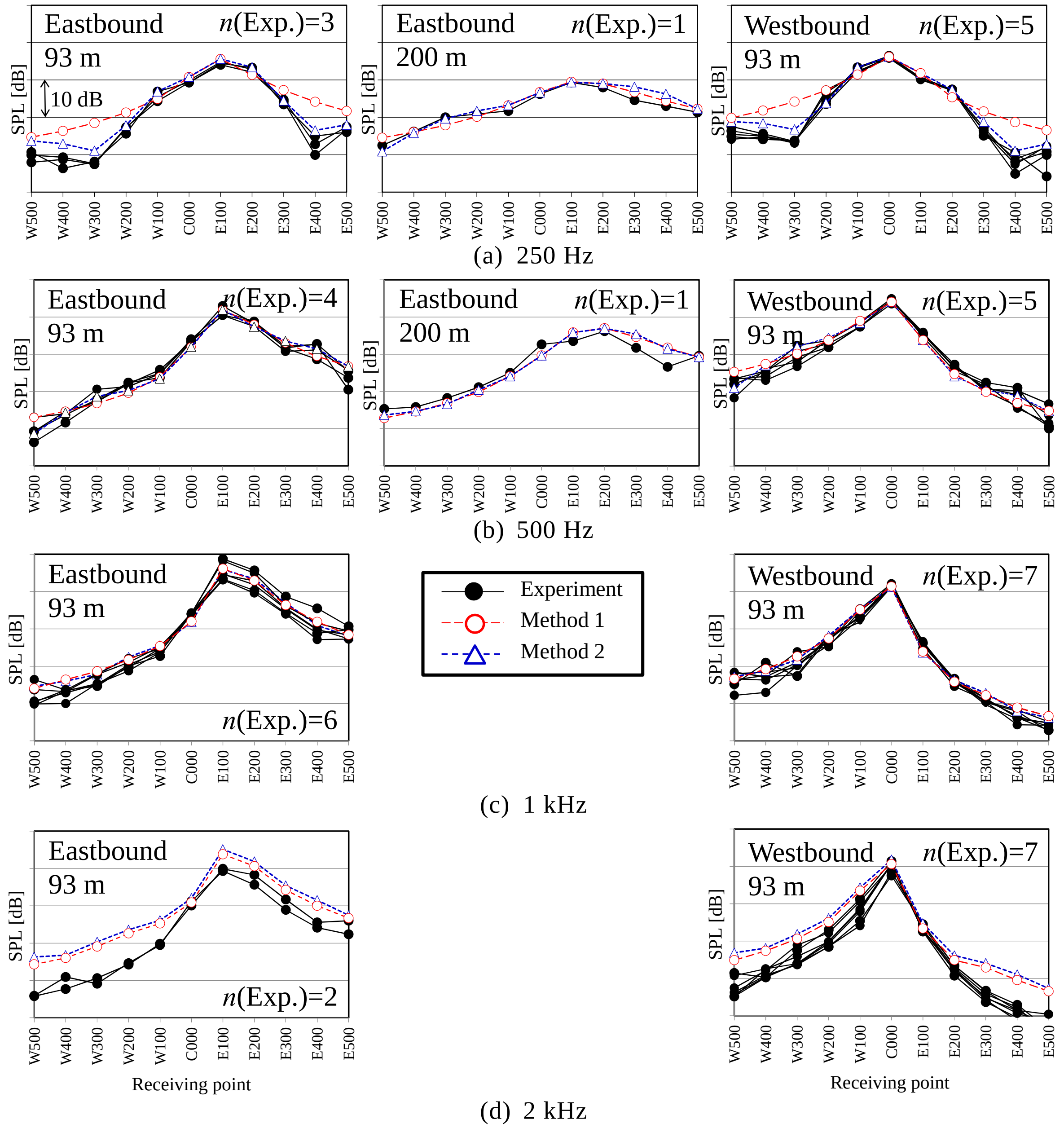

Figure 8 – Comparison of the experimental results with the calculation results by Method 1 and 2.

3.3 Comparison between experiment and calculation

Calculation results are compared with the experimental results in Fig. 8. In this experiment, sound pressure level at a reference distance was back estimated by the levels at receiving points C000, E100 and E200 obtain in this field experiment. For the method 2, sound pressure was calculated at 1/12 octave band center frequencies, and the squared value of the calculated sound pressure were summed up to obtain a 1/1 octave band sound pressure level. For 500 Hz and 1 kHz, calculation results obtained by both methods are in good agreement with the experimental results. In these frequencies, on assessing by 1 octave band level, influence of ground reflection did not appear. To see the results for 250 Hz, obvious difference between the experimental results and the calculation results by the Method 1 can be seen, whereas the difference between the experimental results and the calculation results by the Method 2 is small. In this frequency, sound interference between the direct and reflected sounds considerably affects the sound pressure level at the receiving points, and in such a case, sound propagation should be calculated in wave-base. To see the results for 2 kHz, experimental results on distant receiving points are obviously smaller than the calculation results. At high frequency, atmospheric absorption considerably influences long-range sound propagation, and therefore such an effect may appear in the result.

4. THE GREEN'S FUNCTION PARABOLIC EQUATION METHOD

As a wave-based numerical method of calculating outdoor sound propagation including ground effect by finite impedance of ground and meteorological effects by wind and temperature, a parabolic equation method is often applied. Besides the classical Crank Nicholson parabolic equation (CN-PE) method, the Green's function parabolic equation (GF-PE) method developed by Gilbert and Di (3) is known as a faster implementation of the PE method, in which a spatial range step is allowed to be relatively large. In this study, the GF-PE analysis was applied to the experimental condition performed in this study and the calculation results were compared with the experimental ones. By the GF-PE method, sound field $\phi(r,z)$ are calculated by the following procedure of extrapolation of $\phi(r,z)$ from r to $r+\Delta r$ (3).

$$\phi(r+\Delta r,z)=\exp\left(i\Delta r\frac{\delta k^2(z)}{2k_a}\right)\left\{\frac{1}{2\pi}\int_{-\infty}^{\infty}\left[\Phi(r,k_z)+R(k_z)\Phi(r,-k_z)\right]\exp\left[i\left(\sqrt{k_a^2-k_z^2}-k_a\right)\Delta r\right]\exp(ik_z z)dk_z\right. \\ \left.+2i\beta\Phi(r,\beta)\exp\left[i\left(\sqrt{k_a^2-\beta^2}-k_a\right)\Delta r\right]\exp(-i\beta z)\right\} \quad (4)$$

with

$$\Phi(r,k_z)=\int_0^{\infty}\phi(r,z)\exp(-ik_z z)dk_z\ , \quad (5)$$

where k_a is the wavenumber on the ground, $R(k_z)$ is a plane wave reflection coefficient calculated by $R(k_z)=(k_z Z_g-k_a)/(k_z Z_g+k_a)$ with Z_g as a ground impedance, $\beta=k_a/Z_g$.

4.1 Starting field for a known directionality

To start a spatial marching solution procedure in the PE method, the starting field $\phi(0,z)$ should be specified as the first step. As a conventional method, Gaussian type distribution is often used as a starting field simulating a monopole source as (4),

$$\phi(0,z)=\sqrt{ik_a}\,e^{-k_a^2\frac{(z-z_s)^2}{2}} \qquad \text{for narrow angle PE,} \quad (6)$$

$$\phi(0,z)=\sqrt{ik_a}\left\{1.3717-0.3701k_a^2(z-z_s)^2\right\}e^{-k_a^2\frac{(z-z_s)^2}{2}} \qquad \text{for wide angle PE,} \quad (7)$$

where z_s indicates z-coordinate of a source. In the case where the sound source is directional, other implementation is required. In order to consider the description for the directional point source, here, we start a GF-PE method for a simple sound field without sound refraction in a free field. Then, the spatial marching solution procedure indicated by Eq. (4) can be written by,

$$\phi(r+\Delta r,z)=\frac{1}{2\pi}\int_{-\infty}^{\infty}\Phi(r,k_z)\exp\left[i\sqrt{k_0^2-k_z^2}\Delta r\right]\exp(ik_z z)dk_z\ , \quad (8)$$

with

$$\Phi(r,k_z)=\int_{-\infty}^{\infty}\phi(r,z)\exp(-ik_z z)dk_z\ . \quad (9)$$

On the other hand, according to the plane wave expansion, arbitrary two-dimensional (defined in (r,z) plane) sound field without a source, $p(r,z)$ at a wavenumber k_0, can be expressed as an integration form of plane wave proceeding in all directions as (see Fig.9),

$$p(r,z)=\frac{1}{2\pi}\int_{-\infty}^{\infty}P(k_z)\exp[ik_r\cdot r+k_z\cdot z]dk_z\,, \tag{10}$$

with $k_0^2=k_r^2+k_z^2$,

where k_r=2π/λ_r and k_z=2π/λ_z are components in r- and z-direction of a wavenumber k_0=2π/λ_0, respectively. Here, λ indicates wavelength.

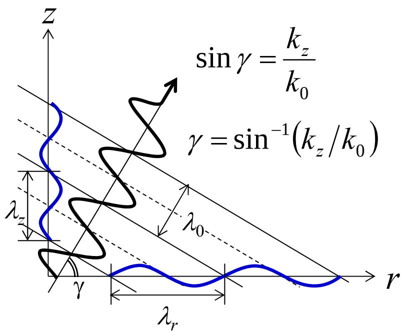

Figure 9 – A plane wave proceeding in a two-dimensional sound field.

Considering $k_r=\sqrt{k_0^2-k_z^2}$ and making r=0 and Δr=r, Eq. (8) is the same form as Eq. (10). Therefore, Eq. (8) for r=0 can be considered as a calculation procedure to obtain a sound field at first range step based on the plane wave expansion. That is,

$$\phi(\Delta r,z)=\frac{1}{2\pi}\int_{-\infty}^{\infty}\Phi(0,k_z)\exp\left[i\sqrt{k_0^2-k_z^2}\Delta r\right]\exp(ik_z z)dk_z \tag{11}$$

$$\Phi(0,k_z)=\int_{-\infty}^{\infty}\phi(0,z)\exp(-ik_z z)dk_z \tag{12}$$

In Eq. (11), $\Phi(0,k_z)$ can be considered as a complex amplitude of a plane wave proceeding in γ direction indicated in Fig. 9. Therefore, when directivity characteristics of a sound source is known as a function $Q(\gamma(k_z))$, by substituting $Q(\gamma(k_z))$ into $\Phi(0,k_z)$ in Eq. (11), sound field generated by the directional sound source can be calculated. Furthermore, substituting Δr=0 and $\Phi(0,k_z)$= $Q(\gamma(k_z))$ in Eq. (11) leads to

$$\phi(0,z)=\frac{1}{2\pi}\int_{-\infty}^{\infty}Q(\gamma(k_z))\exp(ik_z z)dk_z\,, \tag{13}$$

$$\gamma(k_z)=\begin{cases}\sin^{-1}(k_z/k_0) & |k_z|\le k_0\\ 0 & |k_z|>k_0\end{cases}, \tag{14}$$

and this equation is consistent with the inverse Fourier transformation of the function $Q(\gamma(k_z))$. Consequently, the starting field for a directional sound source can be obtained by an inverse Fourier transformation of $Q(\gamma(k_z))$ (5). Practically, an inverse fast Fourier transformation (IFFT) is employed for calculation efficiency (6). As examples of this calculation method, sound pressure distribution for a monopole for wide angle PE method (Eq. (7)) and directivity of the loudspeaker used in this study at 500 Hz and 2 kHz (see Fig. 3) are compared in Fig. 10.

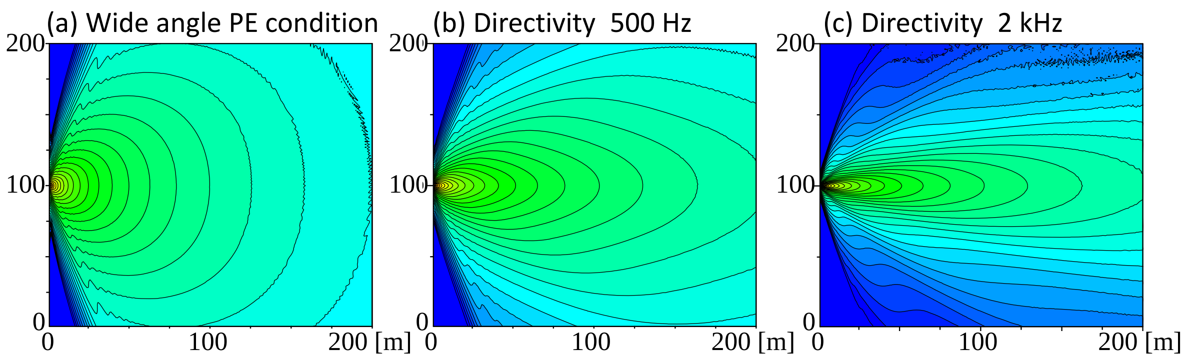

Figure 10 – Sound pressure distribution in a free field.

4.2 Comparison between experiment and GF-PE analysis

The GF-PE calculation was performed under no wind atmospheric condition. Effective sound speed profile was determined by a temperature profile assuming that the temperature gradually decreased with increasing height as $T(z) = T_0 - az$ with T_0 and a as 18.0 ℃ and 0.0065 ℃/m. Acoustic impedance of the ground was given by a regression formula derived by Miki (7) using an effective flow resistivity of 20000 kPa・s/m^2 assuming a hard surface with asphalt. The calculation results are compared with the experimental results in Figure 11. In general, the GF-PE calculation results are in good agreement. In the result for 250 Hz, sound pressure decreasing at W300 and E400 caused by sound interference between the direct path and reflection path via the ground as seen in the section 3.2. The tendency is reproduced in the results by the GF-PE calculation, although a measurable difference was seen between the calculation and experiment appears.

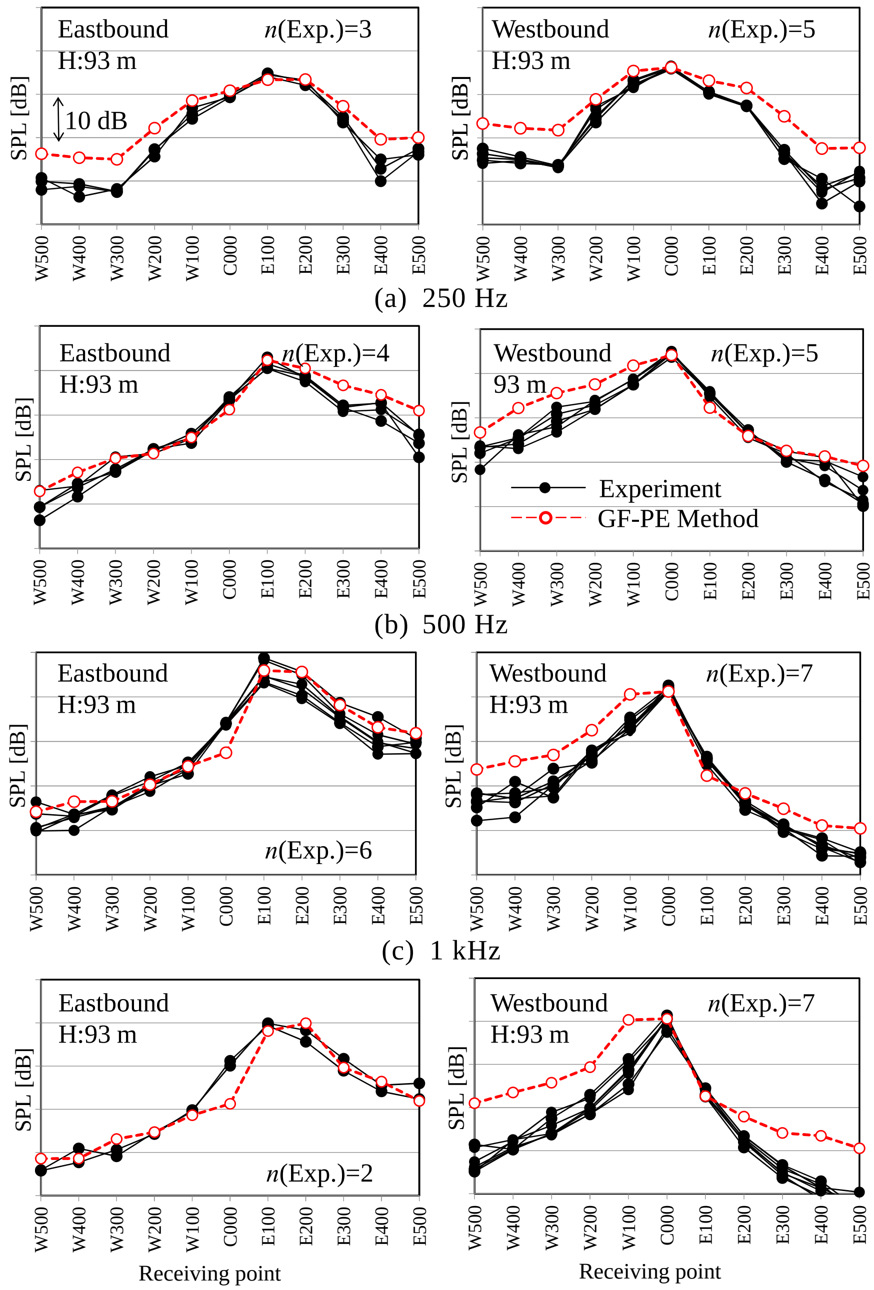

(d) 2 kHz

Figure 11 – Comparison between experiment and GFPE analysis.

Sound pressure distribution calculated by the GF-PE method for 250 Hz and 500 Hz bands are shown in Fig. 12. In the figures, a red circle indicates an elevated point source, and the red lines depict the angle zone $\theta \in [-75,75]$ degrees, out of which the solution is gradually decreased with increasing the angle to stabilize the solution in the GF-PE calculation process. In fact, each distribution map consists of two distribution maps generated by the two directivity conditions of the source, a forward directivity and a backward directivity. The figures show that the directivity characteristics strongly affect the sound pressure distribution.

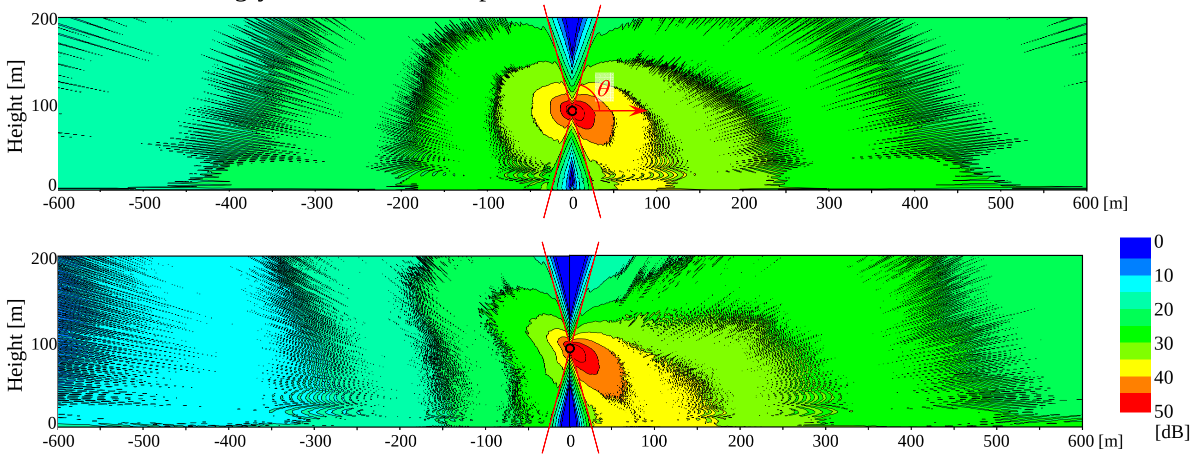

Figure 12 – Sound pressure distribution calculated by the GF-PE method at 250 Hz (upper figure) and 500 Hz (lower figure).

5. CONCLUSIONS

In this study, outdoor sound propagation from an elevated sound source was investigated focusing on the effects of source's directionality. As an experimental investigation, a field experiment was performed using a tethered balloon which lifted up a directional sound source. For calculation method of the sound propagation, simple calculation methods of energy-base and wave-base and the Green's function parabolic equation method were examined. In sound propagation from an elevated source, sound interference between direct sound and reflection sound by ground sometimes affects sound propagation characteristics. Regarding the wave based calculation using the Green's function parabolic equation method, its basic principle calculating sound propagation from a directional sound source was firstly discussed and the calculation results were compared with the experimental results. The calculation results were in good agreement with the experimental ones. The meteorological effects due to wind and temperature affecting to sound propagation from an elevated source should be further investigated

REFERENCES

1. T. Takanashi, S. Sakamoto, S. Yokoyama and H. Ishii. Field experiment on ground-to-ground sound propagation from a directional source. Proc. INTER-NOISE 2014; 16-19 November 2014; Melborne Australia 2014.
2. F. Satoh, J. Hirano, S. Sakamoto and H. Tachibana. Sound propagation measurement using swept-sine signal. Proc. INTER-NOISE 2005; August 2005; Rio de Janeiro, Brazil 2005, No.1691,.
3. K. E. Gilbert and X. Di. A fast Green's function method for one-way sound propagation in the atmosphere. J. Acoust. Soc. Am. 1993; 94(4): 2343-2352.
4. E. M. Solomons. G12 Starting field. In: E. M. Solomons. Computaional atmospheric acoustics. Dordrecht, Netherland: Kluwer Academin Publishers; 2001. p.176-180.
5. S. N. Vecherin and. K. Wilson. Incorporating source directionality into outdoor sound propagation calculations. J. Acoust. Soc. Am. 2011; 130(6): 3608-3622.
6. E. M. Salomons. Improved Green's function parabolic equation method for atmospheric sound propagation. J. Acoust. Soc. Am. 1998; 104 (1): 100-106.
7. Y. Miki. Acoustical properties of porous materials -Modifications of Delany-Bazley models-. J. Acoust. Soc. Jpn. (E) 1990; 11: 19-24.